Search for supernarrow dibaryons via the $pd \rightarrow ppX$ and $pd \rightarrow pdX$ reactions

H. Kuboki,[1,*] A. Tamii,[2] K. Fujita,[2] K. Hatanaka,[2] M. Hatano,[1] J. Kamiya,[3] T. Kudoh,[4] Y. Maeda,[5] K. Sagara,[4] T. Saito,[1] H. Sakai,[1] Y. Sakemi,[2] M. Sasano,[1] K. Sekiguchi,[6] Y. Shimizu,[2] S. Shimomoto,[4] M. Shiota,[4] Y. Tameshige,[2] T. Uesaka,[5] T. Wakasa,[4] and K. Yako[1]

[1]*Department of Physics, The University of Tokyo, Bunkyo, Tokyo 113-0033, Japan*
[2]*Research Center for Nuclear Physics, Osaka University, Ibaraki, Osaka 567-0047, Japan*
[3]*Accelerator Group, Japan Atomic Energy Agency, Tokai, Ibaraki 319-1195, Japan*
[4]*Department of Physics, Kyushu University, Higashi, Fukuoka 812-8581, Japan*
[5]*Center for Nuclear Study, The University of Tokyo, Bunkyo, Tokyo 113-0033, Japan*
[6]*The Institute of Physical and Chemical Research, Wako, Saitama 351-0198, Japan*

(Received 25 March 2006; published 21 September 2006)

Supernarrow dibaryons (SNDs) have been searched for by the $pd \rightarrow ppX$ and $pd \rightarrow pdX$ reactions at $E_p = 295$ MeV over a mass range of 1898 to 1953 MeV, where three candidates of SNDs were found at the Moscow Meson Factory. The experiment was carried out at the Research Center for Nuclear Physics using a two-arm magnetic spectrometer system and a liquid deuterium target. A good mass resolution of 1 MeV and a low background condition were achieved. No resonance structure was observed in the missing mass spectra. Upper limits of the SND production cross section were determined.

DOI: 10.1103/PhysRevC.74.035203 PACS number(s): 13.75.Cs, 14.20.Pt, 12.39.Mk

I. INTRODUCTION

Quantum chromodynamics (QCD) allows for the existence of a variety of six-quark states with a baryon number $B = 2$. Such states are called dibaryons. The observation of dibaryon states provides significant information on the manifestation of QCD effects. Many experiments have been performed to search for dibaryons [1–8]. However no conclusive evidence has been established.

Among many dibaryons we focus on supernarrow dibaryons (SNDs). The SNDs have two characteristics [9]: Firstly, an SND has a symmetric wave function in terms of nucleons, $(-1)^{I+S}\pi = 1$, where I, S, and π are the isospin, the intrinsic spin, and the intrinsic parity of the dibaryon, respectively. The SND cannot decay into a nucleon-nucleon (*NN*) system because of Pauli exclusion principle [10–13]. Secondly, an SND has a mass of less than that of two nucleons and one π meson, $M_D < 2M_N + M_\pi$, where M_D, M_N, and M_π are the masses of the dibaryon, a nucleon, and a pion, respectively. This condition forbids the SND from decaying into the two-nucleon and one π meson system. As a result, the SND decays through only electromagnetic process emitting γ rays with a narrow decay width of less than 1 keV (not MeV) [12]. Since dibaryons which decay by the strong interaction and ordinary *NN* resonances are considered to have broad widths of more than several tens MeV, a narrow width of less than a few MeV would characterize an SND resonance.

A few experiments have been performed to search for SNDs. Khrykin *et al.* found a candidate of an SND at a mass of 1923 MeV via the $pp \rightarrow \gamma D$, $D \rightarrow pp\gamma$ reaction at $E_p =$ 198 MeV, where D denotes an SND, by detecting the emitted two photons in coincidence [14]. However, a subsequent SND search by the *pp* bremsstrahlung reaction at Uppsala performed by Calén *et al.* showed no indication of the candidate [15]. From an additional measurement by Khrykin *et al.* the mass of the candidate was recalibrated to 1956 MeV [16]. Scholten *et al.* theoretically studied possible observation of such dibaryons in the background of two-photon bremsstrahlung [17].

In the *NN* scattering, an SND can be excited only by electromagnetic interaction. Thus the cross section of the SND production is very small. On the other hand, by using three-nucleon scattering, like *pd* scattering, an SND can be excited by the strong interaction. In the latter case, the cross section is expected to be much larger, which significantly increases the experimental sensitivity.

Recently, Fil'kov *et al.* reported candidates of the SNDs in missing mass spectra of the $pd \rightarrow ppX$ reaction at $E_p =$ 305 MeV [18,19]. Two experiments were carried out by employing a proton accelerator at the Moscow Meson Factory (MMF). The missing mass of the $pd \rightarrow pX$ reaction was reconstructed from the data. The scattered proton was detected at angles of 70° and 72.5° in coincidence with the proton from the decay of X by using a two-arm mass spectrometer system. A deuterated polyethylene (C^2H_2) target was used as a deuteron target. The energy information of the scattered protons and the decay particles was obtained by time-of-flight technique together with energy deposits in the detectors. In the first experiment, two narrow peaks in missing mass spectra have been observed at 1905±2 and 1924±2 MeV [18]. Since the widths of the resonances were equivalent to the experimental resolution of 3 MeV, their physical widths had to be less than the experimental resolution. Thus the resonances were attributed to SNDs. The production cross section of the SND at 1905 MeV was estimated to be 8±4 μb/sr on the assumption that the SND mainly decayed into the $pn\gamma$ channel. Later, the cross section was revised to 3±2 μb/sr [20]. In the second experiment, three narrow peaks at 1904±2, 1926±2, and 1942±2 MeV were

*Electronic address: kuboki@nucl.phys.s.u-tokyo.ac.jp

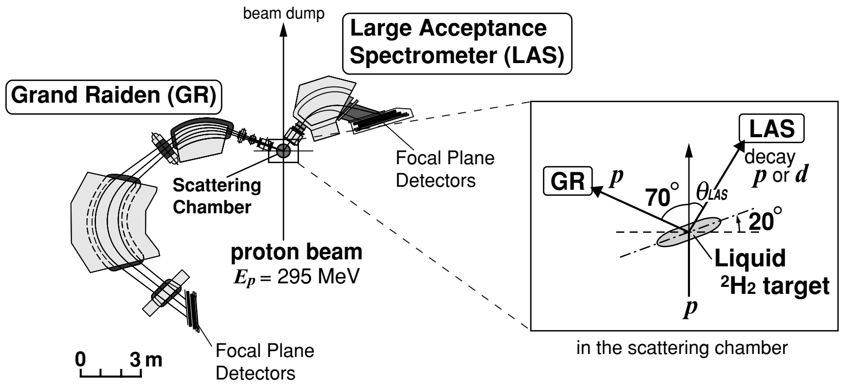

FIG. 1. Overview of the two-arm magnetic spectrometer system, consisting of Grand Raiden (GR) and the Large Acceptance Spectrometer (LAS).

observed [19]. However the spectrum was accompanied by a large number of unknown background events mostly from carbon in the target, and the statistics were very low. The presence of the resonances has been marginal.

Tamii *et al.* performed an SND search experiment for the candidate at 1905 MeV [18] at the Research Center for Nuclear Physics (RCNP) ring cyclotron facility, Osaka University [21]. The kinematical condition was the same as that at the MMF. The measured mass range was from 1896 to 1914 MeV. They employed a C^2H_2 target and a two-arm magnetic spectrometer system. A better mass resolution of 0.95 MeV was achieved. However the resonance peak was not observed. The purpose of this work is to study the existence of the SND candidates over an extended mass range of 1898 to 1953 MeV with higher sensitivity. Background events have been much reduced by employing a liquid deuterium target.

II. EXPERIMENTAL PROCEDURE

The experiment was performed at the RCNP by using a two-arm magnetic spectrometer system. The experimental setup is shown in Fig. 1. A proton beam accelerated up to 295 MeV by the azimuthally-varying-field and ring cyclotrons was transported to the experimental hall, where it bombarded a target in the scattering chamber.

A liquid deuterium target (LDT) [22] was used as a deuteron target. The target cell had beam entrance and exit windows with diameters of 10 and 16 mmϕ, respectively. The windows were sealed by aramid foils with a thickness of 4.4 μm. The thickness of deuterium was 50 mg/cm^2. The thickness of deuterium in the LDT was increased by a factor of 5 than the previously used C^2H_2 target [21], while the thickness of other elements was reduced by more than a factor of 10. The target cell was shielded from heat by an aluminum cylinder. We installed a luminosity monitor [23] in the scattering chamber for monitoring the thickness of the LDT throughout the measurement. Figure 2 shows a schematic view of the luminosity monitor designed to measure the *pd* elastic scattering. The scattered protons and recoil deuterons were detected in kinematical coincidence. The thickness of the LDT changed by ±4% during the measurement because the aramid foils of the target cell swelled in vacuum and bubbles might be produced in the LDT. The C^2H_2 target [24] with a thickness of 44 mg/cm^2 [25] was employed as a deuterium target in order to calibrate the luminosity monitor. The spectra of the C^2H_2 target contained background events from carbon. The spectra were fitted by a Gaussian and a linear background. The background contribution was 2% and was subtracted.

A two-arm magnetic spectrometer system was used to analyze the particle momenta with high accuracy. One of the arms was the Grand Raiden spectrometer (GR) [26], which detected the scattered proton at 70°, the same angle as that of the measurement at the MMF. The other arm was the Large Acceptance Spectrometer (LAS) [27], which detected the SND decay proton (deuteron) in the measurement of the $pn\gamma$ ($d\gamma$) decay channel. The LDT was tilted by 20° toward GR from the normal direction in order to obtain a better scattering-angle resolution by reducing multiple-scattering of the scattered protons. The momentum bite of GR was 5%. The SND mass region of 1898 to 1953 MeV was covered with six magnetic field settings of GR. For each mass region, three magnetic field settings of the LAS were used for the measurement of the $pn\gamma$ decay channel, and one setting for the $d\gamma$ decay channel. The

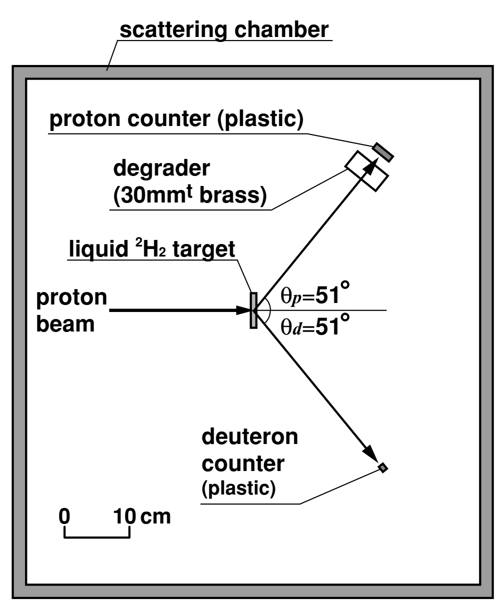

FIG. 2. Schematic view of the luminosity monitor (side view). Two plastic scintillation counters were placed at 51 degrees and at 20 cm from the target. A degrader made of brass with a thickness of 30 mm was used for stopping deuterons from entering the proton counter.

TABLE I. Scattering angles and magnetic field settings of GR and the LAS for the SND search. E_p^c and E_d^c are the central energy of the LAS for the decay protons and deuterons, respectively. Three magnetic field settings, high, medium, and low, were used to detect the decay protons over a wide momentum range for the $pn\gamma$ decay channel. One setting was used for the $d\gamma$ decay channel.

Dibaryon Mass (MeV)	GR		LAS				
	Lab. angle (deg)	Lab. energy E_p (MeV)	Lab. angle (deg)	Lab. energy			
				$pn\gamma$ E_p^c (MeV)			$d\gamma$ E_d^c (MeV)
				High	Medium	Low	
1898–1911	70.0	113.6	35.0	123.7	75.0	48.7	150.8
1909–1921	70.0	105.2	33.7	121.6	73.7	47.8	147.4
1918–1930	70.0	98.2	32.5	119.5	72.4	46.9	144.7
1928–1939	70.0	90.7	31.2	117.2	71.0	46.0	142.0
1937–1946	70.0	83.9	30.0	115.4	69.9	45.3	139.7
1944–1953	70.0	78.7	29.7	114.1	69.1	44.8	138.1

momentum bite of the LAS was 30%. Scattering angles and magnetic field settings of GR and the LAS are summarized in Table I.

III. DATA ANALYSIS

The pd elastic scattering was measured to check the mass resolution of GR at 70°. Figure 3 shows a typical missing mass spectrum of the pd elastic scattering. A mass resolution of 0.96 MeV in full width at half maximum (FWHM) was obtained. The main ingredient of the resolution was the uncertainty of the scattering angle arising from the angular spread of the beam (0.2°) together with the multiple scattering in the target (0.09°) which corresponded to 0.85 MeV. The uncertainty of the missing mass associated with the beam energy spread of 0.20 was 0.12 MeV and the one due to the fluctuation of the energy loss in the target was estimated to be 0.34 MeV.

Software cuts were applied to the momenta and scattering angles measured by GR. The solid angle of GR as a function of the missing mass was essentially the same as that of the previous experiment [21]. The phase space coverage of the decay particles by the LAS was calculated by Monte Carlo simulations for each decay channel by the procedure written in Ref. [21]. The phase space coverage as a function of the missing mass is shown in Fig. 4 for each decay channel.

Spectra of random coincidence events were obtained by putting gates on the time difference between the triggers from the two spectrometers, and were subtracted. A missing mass spectrum for the LDT after subtraction of the random coincidence events is shown in Fig. 5 by the solid curve. The dashed curve is the spectrum of the previous experiment with the C^2H_2 target [28]. It should be noted that the contribution of the background events, mainly due to carbon in the target, was reduced by almost one order of magnitude by using the LDT.

The main sources of the background events were the target cell holder and the heat shield bombarded by a beam halo. Another source was attachment of residual gas on the target cell. These events appeared as a continuum background with

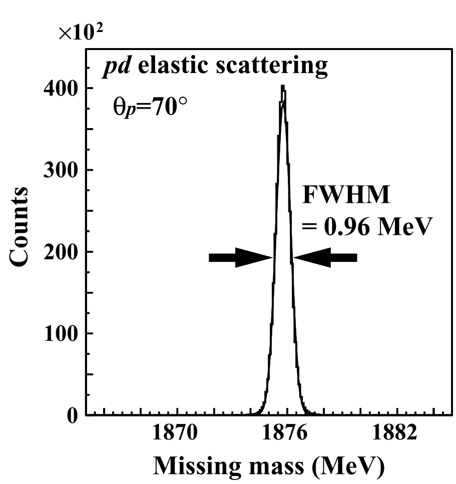

FIG. 3. A missing mass spectrum of the pd elastic scattering. A mass resolution of 0.96 MeV was obtained.

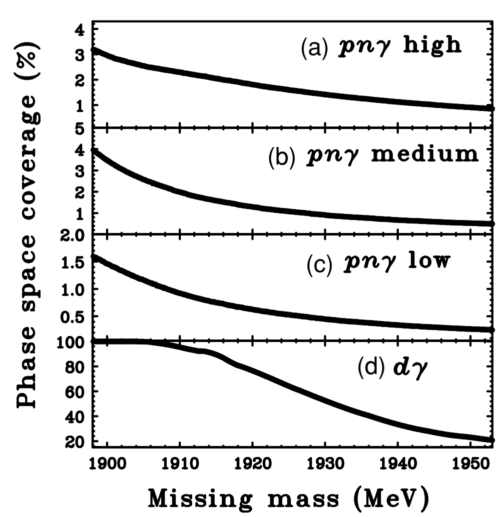

FIG. 4. Phase space coverage of the decay particles by the LAS. (a), (b), and (c) are for the $pn\gamma$ decay channel with the high, medium, and low magnetic fields, respectively. (d) is for the $d\gamma$ decay channel.

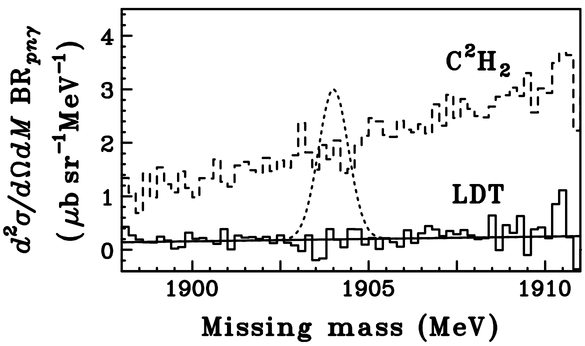

FIG. 5. Missing mass spectra over the mass range of 1898 to 1911 MeV for the $pn\gamma$ decay channel. The horizontal axis is the missing mass and the vertical axis is the SND production cross section multiplied by the branching ratio for the $pn\gamma$ decay channel. The solid and dashed curves represent the spectra of the LDT and the C^2H_2 target [28], respectively. The dotted curve shows the expected dibaryon histogram calculated on the assumption that the differential cross section is 3 μb/sr and the peak width is the same as the experimental resolution. The solid line shows the fitting function to estimate the contribution of the background events.

a flat shape in the missing mass spectra. The dotted curve in Fig. 5 shows the expected dibaryon histogram calculated on the assumption that the differential cross section is 3 μb/sr and the peak width is the same as the experimental resolution. Ratio of the expected signal to the background was 3 to 20 in the measured mass region.

We also performed measurements with the cell in which $^2H_2$ was heated to the gas state. The data were used to check the contribution of the background events due to the target cell. Since it was not practical to keep the experimental conditions of the beam halo and the residual gas stable, the data were not used for subtracting the background events. The background spectra were fitted by a linear function in each mass region (see the solid line in Fig. 5), and was subtracted from the data.

IV. RESULTS

Missing mass spectra after background subtraction are shown in Fig. 6 by solid circles with statistical error bars for the (a) $pn\gamma$ and (b) $d\gamma$ decay channels. The horizontal axis is the missing mass and the vertical axis is the double differential cross section of the SND production multiplied by the branching ratio for the corresponding decay channel. The data shown in Fig. 6(a) are the combined data of the three magnetic fields of the LAS. The solid curves in Fig. 6(a) represent the peaks expected with the experimental resolution of 0.96 MeV on the assumption of the differential cross section of 3 μb/sr and isotropic decay of the dibaryon in its rest frame. The differential cross sections of the peaks at 1926 and 1942 MeV were not reported [19] but they should have values larger than 3 μb/sr, since almost the same number of events were seen compared with the peak at 1904 MeV in their spectrum though the angular acceptance of the spectrometer became smaller as the missing mass became larger. The

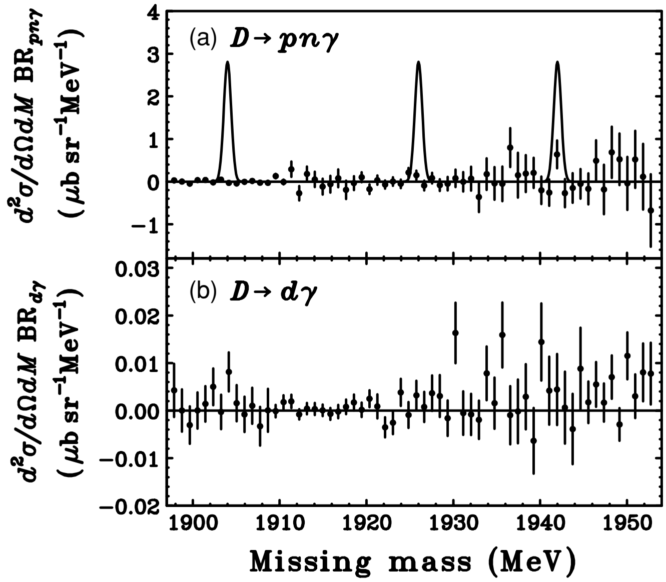

FIG. 6. Double differential cross section of the SND production multiplied by the branching ratio for the (a) $D \rightarrow pn\gamma$ and (b) $D \rightarrow d\gamma$ decay channels, where D denotes an SND. The data of this experiment are plotted by solid circles with statistical error bars. The solid curves represent the expected histograms of the data by Fil'kov *et al.* [18–20] on the assumptions of a differential cross section of 3 μb/sr and isotropic decay of the dibaryon in its rest frame.

maximum standard deviation for the presence of a narrow peak is 2.7 which was obtained by a statistical calculation on the assumption of a peak width from 0.9 to 5.4 MeV in the whole measured mass region [29]. We conclude that no resonance has been observed within the experimental sensitivity.

The upper limit of the SND production cross section at the 90% confidence level (CL) was calculated according to the procedure described in Refs. [30,31]. The following probability density function G of a Gaussian shape is used for each 1.2 MeV mass bin;

$$G(\mu|Y) = \frac{\frac{1}{\sqrt{2\pi}\sigma}\exp\left(-\frac{(Y-\mu)^2}{2\sigma^2}\right)}{\int_0^\infty \frac{1}{\sqrt{2\pi}\sigma}\exp\left(-\frac{(Y-\mu)^2}{2\sigma^2}\right)d\mu}(\mu \geqslant 0), \qquad (1)$$

where Y is the observed yield in the bin, σ is its statistical error, and μ is the true value. Since the production cross section must be positive or zero, Eq. (1) is defined in the region of $\mu \geqslant 0$. The bin width of 1.2 MeV is optimum for getting the lowest upper limit, which was determined from the experimental resolution of 0.96 MeV. The upper limit (μ_0) at the mass of the bin is determined as it satisfies

$$\int_0^{\mu_0 \times 0.86} G(\mu|Y)d\mu = 0.90. \qquad (2)$$

If an SND peak has a Gaussian shape with the experimental resolution of 0.96 MeV (FWHM), the fraction of the Gaussian distribution contained in the central 1.2 MeV region is 0.86. This factor is included in Eq. (2). The upper limits obtained are plotted as a function of the missing mass in Fig. 7 for the (a) $pn\gamma$ and (b) $d\gamma$ decay channels. The datum at 1904 MeV of the MMF experiment is shown with a dagger in Fig. 7.

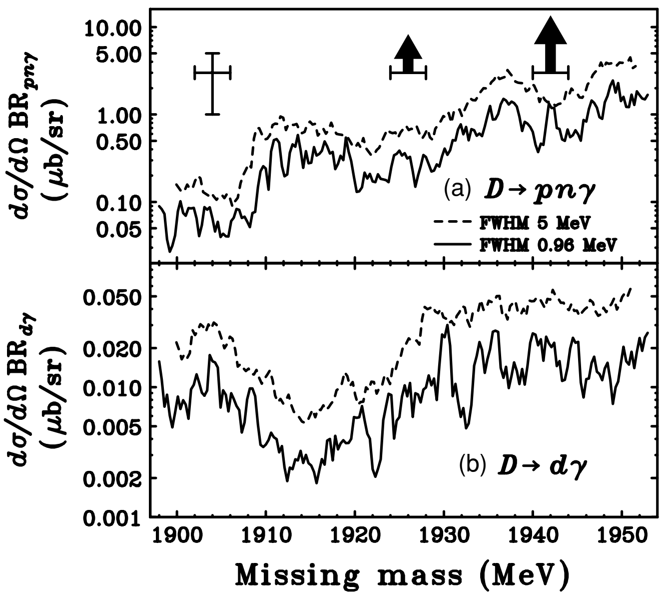

FIG. 7. Upper limits of the SND production cross section at the 90% CL as a function of the missing mass for the (a) $D \rightarrow pn\gamma$ and (b) $D \rightarrow d\gamma$ decay channels, where D denotes an SND. The solid curves represent the upper limits on the assumption that the decay width of an SND is much smaller than the experimental resolution. The dagger at 1904 MeV represents the SND production cross section of 3 ± 2 μb/sr reported in Ref. [20]. The cross sections of the candidates at 1926 and 1942 MeV of Ref. [19] should be larger than 3 μb/sr. The dashed curves represent the upper limits on the assumption that the width of an SND peak is 5 MeV, which corresponds to the mass resolution of the MMF experiment [19].

Those for the peaks at 1926 and 1942 MeV should be larger than 3 μb/sr. The upper limits are small enough to exclude the candidates of SNDs observed at the MMF experiment. The upper limits are also calculated on the assumption that an SND peak width is 5 MeV, which corresponds to the experimental resolution of the MMF experiment. The obtained upper limits are plotted in Fig. 7 by the dashed curves. The upper limits are found to be smaller than the data observed in the MMF experiment. We conclude that the SND candidates with a width of 5 MeV are also excluded.

V. SUMMARY

We measured the $pd \rightarrow ppX$ and $pd \rightarrow pdX$ reactions at $E_p = 295$ MeV to search for SND resonances over the mass range of 1898 to 1953 MeV, where three candidates were reported [18,19]. We obtained a good mass resolution of 0.96 MeV by using a two-arm magnetic spectrometer system. The background was reduced by more than a factor of ten comparing with the previous SND search experiment [21] by using a liquid deuterium target system. The obtained missing mass spectra were flat showing no resonance structure within the statistical accuracy for each decay channel. The upper limits of the SND production cross section at the 90% CL were determined from the data for each decay channel. The SND candidates observed in the MMF experiment [19] have been excluded.

ACKNOWLEDGMENTS

We are grateful to the RCNP cyclotron crew for the excellent proton beam. We also want to acknowledge L.V. Fil'kov for useful discussions. This experiment was performed under the Program No. E196 at the RCNP.

[1] E. Doroshkevich *et al.*, Eur. Phys. J. A **18**, 171 (2003).
[2] P. A. Żołnierczuk, T. P. Gorringe, M. D. Hasinoff, M. A. Kovash, S. Tripathi, and D. H. Wright, Phys. Lett. **B549**, 301 (2002).
[3] T. A. Armstrong *et al.*, Phys. Rev. C **63**, 054903 (2001).
[4] K. Wijesooriya *et al.*, Phys. Rev. Lett. **86**, 2975 (2001).
[5] F. Merrill *et al.*, Phys. Rev. C **63**, 035206 (2001).
[6] B. Tatischeff, J. Yonnet, M. Boivin, M. P. Comets, P. Courtat, R. Gacougnolle, Y. Le Bornec, E. Loireleux, F. Reide, and N. Willis, Phys. Rev. C **59**, 1878 (1999).
[7] H. Clement *et al.*, Prog. Part. Nucl. Phys. **36**, 369 (1996).
[8] M. P. Locher, M. E. Sainio, and A. Svarc, Adv. Nucl. Phys. **17**, 47 (1986).
[9] L. A. Kondratyuk, B. V. Martem'yanov, and M. G. Shchepkin, Sov. J. Nucl. Phys. **45**, 776 (1987).
[10] P. J. Mulders, A. T. Aerts, and J. J. de Swart, Phys. Rev. D **21**, 2653 (1980).
[11] L. V. Fil'kov, Sov. J. Nucl. Phys. **47**, 437 (1988).
[12] D. M. Akhmedov and L. V. Fil'kov, Nucl. Phys. **A544**, 692 (1992).
[13] S. B. Gerasimov, S. N. Ershov, and A. S. Khrykin, Phys. At. Nucl. **58**, 844 (1995).
[14] A. S. Khrykin *et al.*, in Proceedings of the VII International Conference on Meson-Nucleon Physics and the Structure of the Nucleon, TRIUMF, Vancouver, 1997 (unpublished).
[15] H. Calén *et al.*, Phys. Lett. **B427**, 248 (1998).
[16] A. S. Khrykin, V. F. Boreiko, Yu. G. Budyashov, S. B. Gerasimov, N. V. Khomutov, Yu. G. Sobolev, and V. P. Zorin, Phys. Rev. C **64**, 034002 (2001).
[17] O. Scholten, J. G. O. Ojwang, and S. Tamenaga, Phys. Rev. C **71**, 034005 (2005).
[18] L. V. Fil'kov, V. L. Kashevarov, E. S. Konobeevski, M. V. Mordovskoy, S. I. Potashev, and V. M. Skorkin, Phys. Rev. C **61**, 044004 (2000).
[19] L. V. Fil'kov, V. L. Kashevarov, E. S. Konobeevski, M. V. Mordovskoy, S. I. Potashev, V. A. Simonov, V. M. Skorkin, and S. V. Zuev, Eur. Phys. J. A **12**, 369 (2001).
[20] L. V. Fil'kov (private communication).
[21] A. Tamii, K. Hatanaka, M. Hatano, D. Hirooka, J. Kamiya, H. Kato, Y. Maeda, T. Saito, H. Sakai, S. Sakoda, K. Sekiguchi, N. Uchigashima, T. Uesaka, T. Wasaka, and K. Yako, Phys. Rev. C **65**, 047001 (2002).
[22] K. Sagara, H. Akiyoshi, T. Fujita, T. Bussaki, K. Tsuruta, and T. Maeda, RCNP Annual Report, 1995, p. 158.

[23] H. Kuboki, A. Tamii, H. Sakai, and K. Sagara, RCNP Annual Report, 2002, p. 131.
[24] Y. Maeda, H. Sakai, K. Hatanaka, and A. Tamii, Nucl. Instrum. Methods Phys. Res. A **490**, 518 (2002).
[25] K. Hatanaka, Y. Shimizu, D. Hirooka, J. Kamiya, Y. Kitamura, Y. Maeda, T. Noro, E. Obayashi, K. Sagara, T. Saito, H. Sakai, Y. Sakemi, K. Sekiguchi, A. Tamii, T. Wakasa, T. Yagita, K. Yako, H. P. Yoshida, V. P. Ladygin, H. Kamada, W. Glöckle, J. Golak, A. Nogga, and H. Witała, Phys. Rev. C **66**, 044002 (2002).
[26] M. Fujiwara, H. Akimune, I. Daito, H. Fujimura, Y. Fujita, K. Hatanaka, H. Ikegami, I. Katayama, K. Nagayama, N. Matsuoka, S. Morinobu, T. Noro, M. Yoshimura, H. Sakaguchi, Y. Sakemi, A. Tamii, and M. Yosoi, Nucl. Instrum. Methods Phys. Res. A **422**, 484 (1999).
[27] N. Matsuoka, T. Noro, K. Sagara, S. Morinobu, A. Okihana, and K. Hatanaka, RCNP Annual Report, 1991, p. 186.
[28] A. Tamii (private communication).
[29] B. Tatischeff, M. P. Combes-Comets, P. Courtat, R. Gacougnolle, Y. Le Bornec, E. Loireleux, F. Reide, N. Willis, A. M. Bergdolt, G. Bergdolt, O. Bing, F. Hibou, M. Boivin, and A. Moalem, Phys. Rev. C **45**, 2005 (1992).
[30] O. Helene, Nucl. Instrum. Methods **212**, 319 (1983).
[31] Particle Data Group, R. M. Barnett *et al.*, Phys. Rev. D **54**, 1 (1996).